

Modeling the Field Control of the Surface Electroclinic Effect and its Impact on Smectic Layer Strain

Kara Zappitelli; karazapp@gmail.com,
Department of Physics
California Polytechnic State University,
San Luis Obispo, CA 93407
United States

©2014 Zappitelli, K.

June 11, 2014

Abstract

Chiral, smectic liquid crystal molecules align in layers and can be controlled by the application of an electric field, yielding a variety of implications for the quality of liquid crystal (LC) displays. Both the bulk electroclinic effect (BECE) and surface electroclinic effect (SECE) impact the angle at which the molecules tilt with respect to the layer normal in different areas of a LC cell due to dipole interactions. Certain LC's exhibit a continuous Sm-A* to Sm-C* transition, where the angles of the surface and bulk molecules change continuously with electric field strength. Other LC's exhibit first order transitions where we see jumps in the tilt magnitude and hysteresis at different values of the applied electric field. The difference in angle of the bulk and surface molecules in both of these situations causes discrepancies in the layer spacing within the LC cell. These discrepancies lead to frustrations within the cell that can be quantified by strain. These frustrations can be relieved in a number of ways, however the method of relief may lead to negative impacts on the alignment quality of the display itself. Here, we first investigate the BECE and SECE separately and then later consider the effects simultaneously. We then present qualitative representations of this phenomenon and aim to explain significant decreases in alignment quality seen experimentally for particular values of applied electric field.

Contents

1	Liquid Crystals: An Introduction	4
2	Smectic-A to Smectic-C Transition	5
2.1	Analyzing Fixed Points	6
2.1.1	Continuous Transition	7
2.1.2	First Order Transition	7
3	The Bulk Electroclinic Effect	15
3.1	Continuous BECE	17
3.2	First Order BECE	18
4	The Surface Electroclinic Effect	19
4.1	The Euler - Lagrange Equation	21
4.2	θ_S vs. w	22
5	Field Control of the SECE	24
5.1	Continuous Transition	25
5.2	First Order Transition	25
6	Layering Effects	26
6.1	A Qualitative Analysis of the Continuous Transition	26
6.1.1	$E \leq 0$	27
6.1.2	$E \geq E_0$	27
6.1.3	$0 < E < E_0$	28
7	Strain: Quantifying Layer Effects	29
	References	33

1 Liquid Crystals: An Introduction

While we encounter liquid crystals on a daily basis - in our smart phones, computer screens, TVs, etc. - not many people truly appreciate the intricacy of this special phase of matter. The phases of matter familiar to most are the solid, liquid, and gas, however these are certainly not the only phases of matter. Liquid crystals are an intermediate phase present in certain materials between the solid and liquid phase. They display an intermediate amount of order. Molecules within a solid are essentially fixed in place and fixed in orientation. The molecules within a liquid, however, are not fixed in place and are free to move about with whichever orientation they prefer. Liquid crystals are able to preserve the orientational order of a solid but are similar to a liquid in that they lack significant positional order and are free to move about. The presence of orientational order within a liquid crystal is due to their elongated molecular structure. This elongated structure causes the molecules to, on average, align their long axes in the same direction. This average orientation can be described by an arrow called the director, which points along the direction of preferred orientation [1]. Refer to Fig. (1) for clarity.

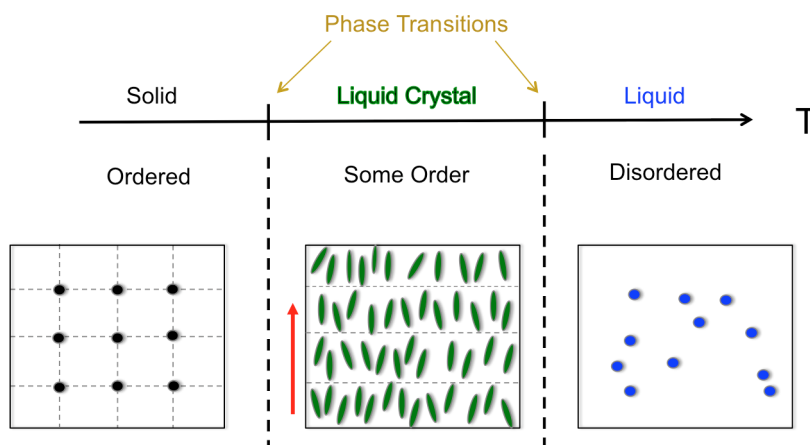


Figure 1: Liquid crystals are an intermediate phase of matter between a solid and liquid. They display orientational but not positional order.

There are many different types of liquid crystals. The type we will be concerned with in this paper are thermotropic liquid crystals, which occur in specific temperature ranges. These types of liquid crystals often display different subphases within the liquid crystal phase based on temperature as well. In the nematic phase, the molecules display orientational but no positional order. If the temperature is lowered, however, the smectic phase can be induced. In the smectic phase, the molecules tend to align along the same direction and they tend to organize themselves in layers, therefore displaying slight positional order [1]. Fig. (1) shows a smectic liquid crystal. It is the intricacies of the smectic phase that will be studied in detail over the course of this paper.

2 Smectic-A to Smectic-C Transition

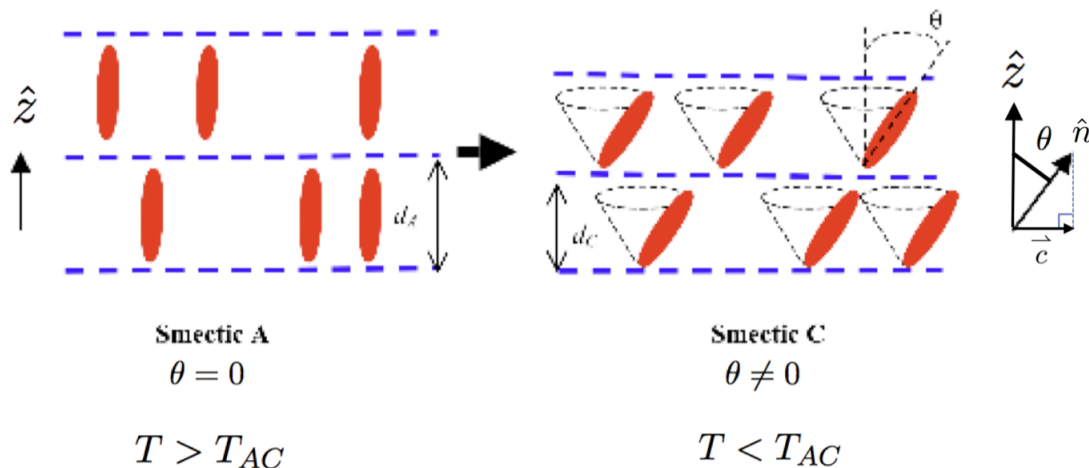


Figure 2: On the left is a visual depiction of a liquid crystal in the Sm-A phase and on the right is a visual depiction of the Sm-C phase. On the far right, there is a geometrical interpretation of the order parameter vector \vec{c} .

Smectic liquid crystals in the A-phase (Sm-A) have an average molecular tilt of zero with respect to the z-axis. A C-phase smectic (Sm-C) occurs when the average molecular tilt is non-zero. This transition can be induced by a temperature decrease below a critical temperature in the cell containing the molecules. A schematic of this transition can be seen in Fig. (2). The order parameter used to characterize the tilting of the molecules is the vector \vec{c} , which is the projection of the tilt on to the layer and is given by $\sin(\theta)$. The actual tilting of the molecule with respect to the z-axis is thus given by $\theta = \sin^{-1}(c)$. The total free energy in a liquid crystal cell is modeled using the Landau Free Energy Equation:

$$F = \int \delta x \delta y \delta z \left[\frac{1}{2} r(T) c^2 + \frac{1}{4} u c^4 + \frac{1}{6} v c^6 \right] = V f(c), \quad (1)$$

where V is the volume of the system and $f(c)$ is used to model the free energy density of liquid crystal molecules in the absence of an electric field and is the following:

$$f(c) = \frac{1}{2} r(T) c^2 + \frac{1}{4} u c^4 + \frac{1}{6} v c^6. \quad (2)$$

The parameter r denotes a function of T which is proportional to the percentage above the transition temperature. $r(T) = A\tau(T)$ where $\tau(T) = (T - T_c)/T_c$ and T_c is the transition temperature. A is a proportionality constant. It is this parameter that directly

affects the tilting of the molecules when temperature is varied, as a bifurcation in the system's stability will occur when temperature is lowered beyond T_c . In this section, we use r to describe the behavior of the system, but later on we will use τ for a more qualitative, experimental investigation. The tilting is represented by the order parameter c where $c \neq 0$ characterizes the Sm-C transition. In a more advanced analysis, the magnitude and direction of the vector \vec{c} is accounted for, but for our purposes we analyze only the magnitude of the tilt. The parameter u dictates which type of transition will occur and how the fixed points of the system will bifurcate. When $u > 0$, a continuous transition will occur. When $u < 0$ a first order transition will occur. We use this form of the energy for a number of reasons. Since energetically it does not matter which way the molecules tilt with respect to the z-axis, we do not include odd powers of c to avoid the impact of sign changes. We only include enough even powers to stabilize the system so that the tilt settles to a finite value. When u is negative, we must include up to 6th order. When u is positive, the sixth order term can be neglected.

An important implication of the Sm-A to Sm-C transition is the impact that it has on the preferred layer spacing of the system. In the Sm-A phase, the molecules have zero tilt and thus prefer a larger layer spacing. In the Sm-C phase, the molecules are tilted with respect to the layer normal which results in a smaller preferred layer spacing throughout the whole system. This phenomenon is illustrated in Fig. (3). The implications of these preferred layer spacing changes in a Sm-A to Sm-C transition will be investigated in further detail towards the end of this paper.

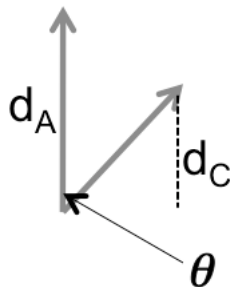


Figure 3: The molecules in a liquid crystal cell have a smaller preferred layer spacing d_C in the Sm-C phase than the larger spacing in the Sm-A phase, d_A .

2.1 Analyzing Fixed Points

By analyzing the fixed points of the system, we can gain insight into the stability changes of the tilting as the temperature fluctuates. As f is an energy, we can obtain an expression for \dot{c} using $\dot{c} = -\frac{df}{dc}$:

$$\dot{c} = -(rc \pm uc^3 + vc^5),$$

where the + corresponds to a value of $u > 0$ and the - corresponds to a value of $u < 0$.

2.1.1 Continuous Transition

Starting with the more simple case where $u > 0$, we can solve for the fixed points of the system by setting $\dot{c} = 0$ and solving for c_* . As stated above, the 6th order term can be ignored since it is working in unison with the 4th order term. Thus, \dot{c} becomes

$$\dot{c} = -rc_* - uc_*^3 = 0.$$

Solving this equation yields the following fixed point values of c_* :

$$c_* = 0, c_* = \pm\sqrt{-r/u}.$$

The fixed point at $c_* = 0$ will exist for all values of r but is only stable for $r > 0$, and the fixed points at $c_* = \pm\sqrt{-r/u}$ will only exist for values of $r < 0$, since $u > 0$. For $r > 0$, the origin is the only stable fixed point, as seen in Fig. (4).

This can be further seen in Fig. (5) by plotting \dot{c} vs. c and looking at where the graph crosses the origin, or where $c = c_*$. For $r > 0$, the graph crosses the x-axis only once at the origin. Since the slope is negative at this point, this means that there is a stable fixed point at this value of c . When $r < 0$, the graph crosses the x-axis at three separate points, once at the origin and once on either side. The graph has negative slope where it crosses the x-axis not at the origin, corresponding to the wells in Fig. (4) and the fixed points of $c_* = \pm\sqrt{-r/u}$. As soon as r becomes negative, the fixed point at the origin becomes unstable as seen by the positive slope at this point.

The situation where $u > 0$ is a continuous phase transition. Consider dialing down r from a positive value to a negative value. At $r = 0$, a supercritical pitchfork bifurcation occurs and immediately it becomes more energetically favorable for the molecules within the liquid crystal cell to begin tilting. Under these circumstances, the nonzero fixed points are stable. The value of r where the molecules begin to tilt is called the threshold value of r , and it corresponds to the transition temperature T_c . In this case the threshold value is $r = 0$ and the behavior can be seen in the bifurcation diagram in Fig. (6). In general, the system as a whole will be only in the Sm-A phase for a value of $r > 0$ and only in the Sm-C phase for $r < 0$. This is illustrated simply by the phase diagram in Fig. (7).

2.1.2 First Order Transition

It is now time to look at the more complicated case, where $u < 0$. Under these circumstances, changing the value of r has an even more radical effect. This results in a first order transition where the molecules in the liquid crystal cell will jump to a preferred

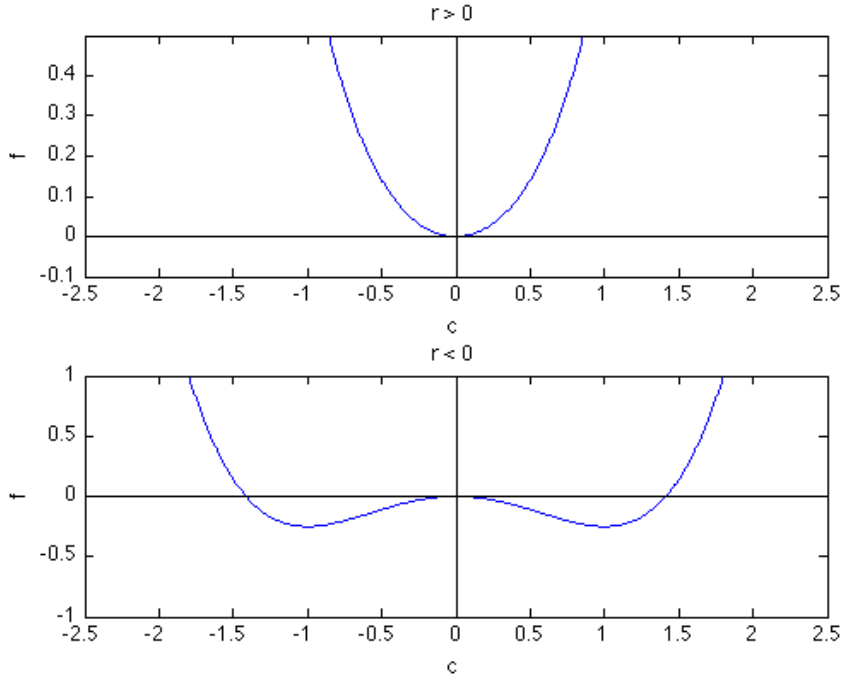


Figure 4: Above are the graphs of the free energy vs. the tilting of the molecules for different values of $r(T)$. For graphical purposes, $u = +1$. On top is the graph of f when $r = 0$, which only has one possible angle of tilt at the origin. On the bottom is the graph of f when $r < 0$, or $T < T_c$. In this case, there are three possible values of c_* , corresponding to the three fixed points found earlier. These fixed points are the extrema of the energy function.

value of tilt at a threshold value of r . In this situation, we are no longer able to ignore the sixth order term so equation (2.1) now becomes:

$$\dot{c} = -rc + uc^3 - vc^5.$$

where $v > 0$. As before, the equation for \dot{c} must be set equal to zero and then the fixed points of the system can be solved for.

$$\begin{aligned} \dot{c} &= -rc_* + uc_*^3 - vc_*^5 \\ &= c_*(-r + uc_*^2 - vc_*^4) = 0. \end{aligned}$$

This yields $c_* = 0$ and $-r + uc_*^2 - vc_*^4 = 0$, giving one fixed point at $c_* = 0$ and allowing us to solve for the next fixed points:

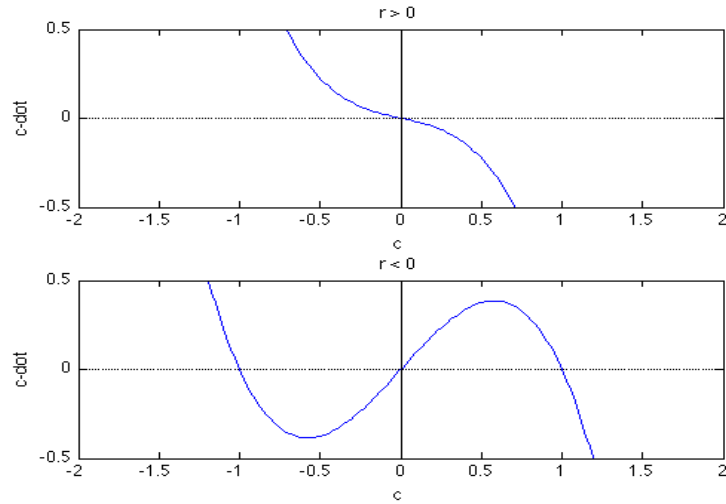


Figure 5: This figure shows \dot{c} vs. c when $u = +1$. When $\dot{c} = 0$, the values of c_* are obtained. The slope at each point where the graph crosses the x-axis indicates the stability of the fixed point. For $r < 0$, there are two stable fixed points and one unstable. For $r > 0$, there is only one stable fixed point at the origin.

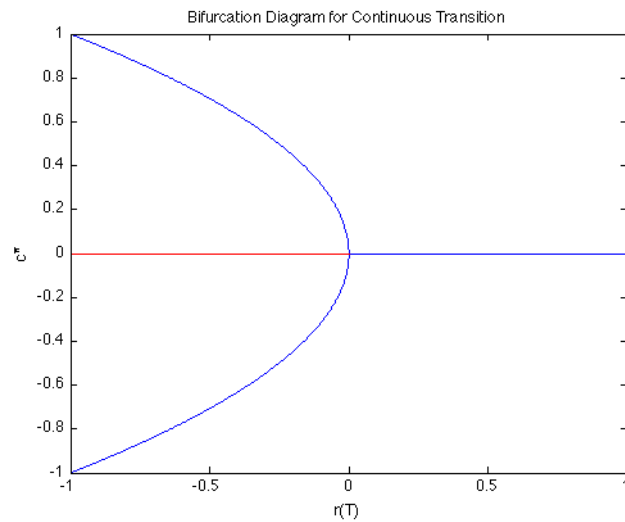


Figure 6: The fixed points plotted as a function of r for the continuous phase transition. The blue lines correspond to stable fixed points and the red corresponds to unstable fixed points. The value of r where the bifurcation occurs is directly related to the transition temperature, T_c , of the liquid crystal.

$$\begin{aligned}
 -r + uc_*^2 - vc_*^4 &= 0 \\
 \varphi_* &= c_*^2 \\
 -r + u\varphi_* - v\varphi_*^2 &= 0
 \end{aligned}$$



Figure 7: For a value of $r > 0$, the system can only be in the Sm-A phase. To be in the Sm-C phase, r must be less than zero.

Applying the quadratic formula yields:

$$\varphi_* = \frac{u \pm \sqrt{u^2 - 4rv}}{2v}.$$

Since $\varphi_* = c_*^2$ then,

$$c_*^2 = \frac{u \pm \sqrt{u^2 - 4rv}}{2v},$$

$$c_* = \pm \sqrt{\frac{u \pm \sqrt{u^2 - 4rv}}{2v}}.$$

The result of this calculation is the appearance of five possible fixed point values of c_* for $u < 0$. However, by changing the value of r , some of the fixed points will appear or disappear and their stability will change. For clarity, each fixed point will be discussed with respect to r in Table (1) and their changing stability will be addressed in Fig. (9). In order to picture this situation graphically, as was done for the continuous transition, it is important to look at the free energy vs. c graphs for varying values of r . Refer to Fig. (8). The fixed points for each value of r correspond to the minimums and maximums of the energy. This idea is further seen in Fig. (9), where \dot{c} vs. c is plotted. These are the phase portraits of the system. Conclusions can also be made about the changing stability of the fixed points. By looking at where the phase plots cross the x-axis, the slope at each fixed point can be determined. If that slope is negative, that fixed point is stable. If the slope is positive, the fixed point is unstable.

Due to the appearance and disappearance of fixed points in the first order transition, it is useful to investigate the bifurcation diagram seen in Fig. (10). As r is dialed down, we see the appearance of four new fixed points at r_c or at the transition temperature T_c .

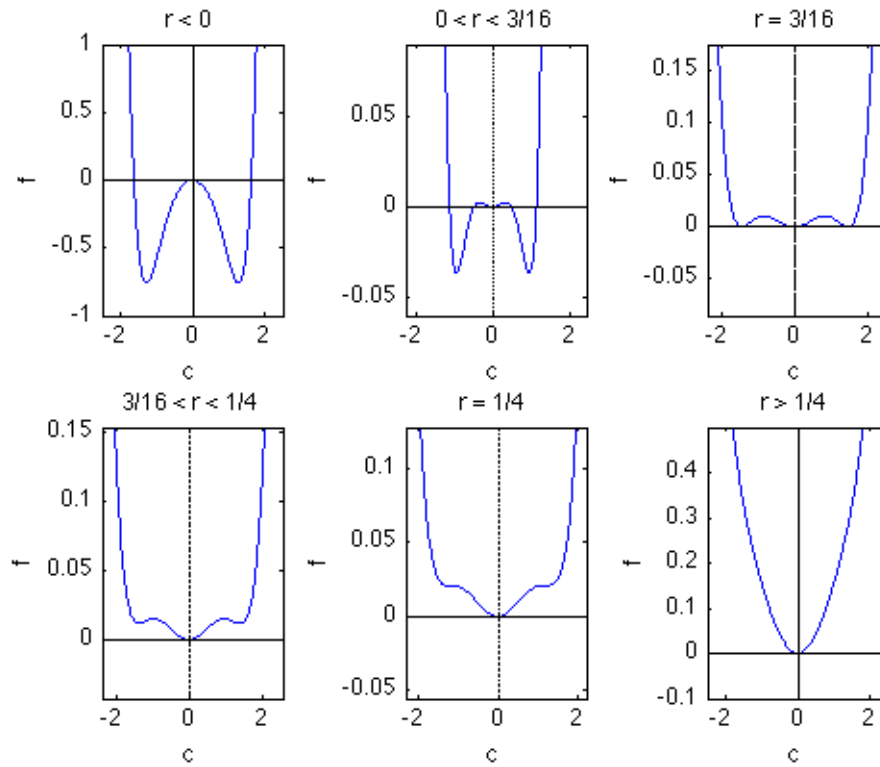


Figure 8: This figure shows the free energy vs. c for varying r values, as discussed in Table (1). For simplicity, $u = -1$ and $v = 1$. The peaks and wells of the free energy correspond to the individual fixed points of the system. By varying r , it is shown that fixed points appear and reappear.

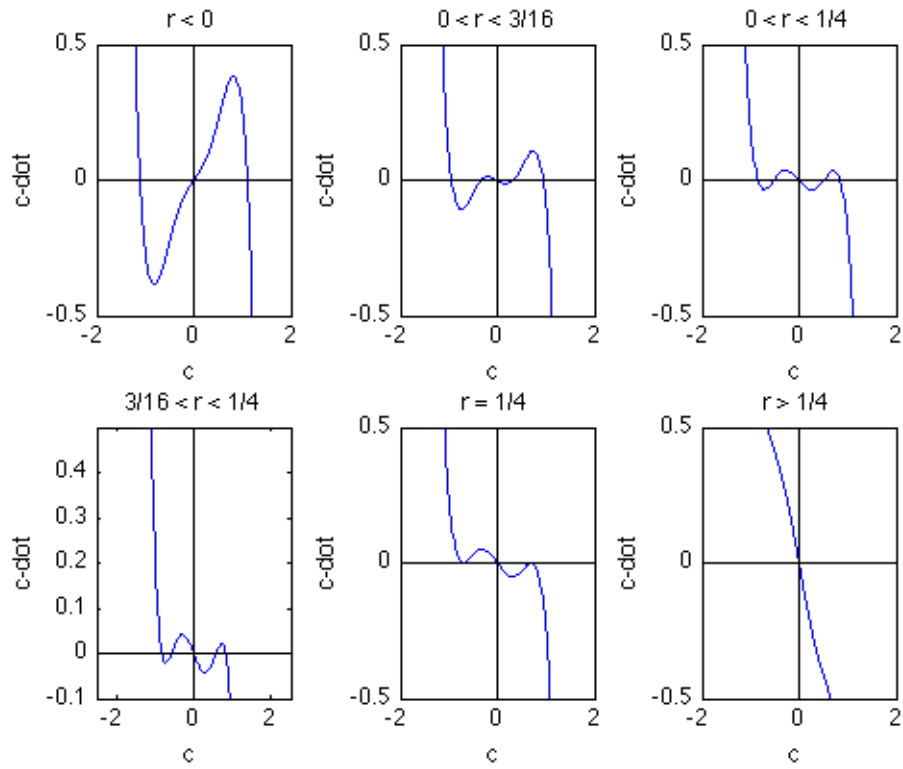


Figure 9: This figure shows \dot{c} vs. c for the first order transitions. For simplicity, $u = -1$ and $v = 1$. The points at which the graphs cross the x-axis correspond to the fix points of the system for that value of r . The stability is given by the slope of the line at those points. Negative slope corresponds to stable fixed points and positive to unstable fixed points.

$r < 0$	$\sqrt{\frac{u-\sqrt{u^2-4rv}}{2v}}$ not real. Fixed points are $c_* = \pm\sqrt{\frac{u+\sqrt{u^2-4rv}}{2v}}$ and $c_* = 0$.
$r = 0$	3 Possible Fixed Points: $c_* = 0, \pm\sqrt{\frac{u}{v}}$
$0 < r < \frac{u^2}{4v}$	5 Possible Fixed Points: $c_* = 0, \pm\sqrt{\frac{u \pm \sqrt{u^2-4rv}}{2v}}$
$r = \frac{u^2}{4v}$	3 Possible Fixed Points: $c_* = 0, \pm\sqrt{\frac{u}{2v}}$
$r > \frac{u^2}{4v}$	$\sqrt{u^2 - 4rv}$ is not real. Only one possible fixed point: $c_* = 0$

Table 1: The above table shows the available fixed points for the first order transition as the parameter r varies. As one can see, fixed points emerge and are annihilated as r is ramped up and down. The value of $\frac{u^2}{4v}$ is known as r_c , and is the r value corresponding to the critical temperature. Further clarification can be seen graphically in Fig. (8 and 9).

In contrast to the continuous transition discussed above, the molecules will experience an instantaneous jump in tilt from zero to nonzero at some critical temperature, characteristic of a subcritical pitchfork bifurcation. As seen in the figure, there is a region between $r = 0$ and $r = r(T_c)$ where two different stable states coexist. This allows for the possibility of hysteresis, meaning that the transition may not always occur at an exact value of T_c , but will depend on the initial conditions of the system.

To better understand the behavior of this hysteresis, it is useful to think about the phase transition in a one dimensional phase diagram, seen in Fig. (11). For sufficiently large values of r , the system is in an entirely Sm-A phase. Once we reach the critical value of r_c , two new minimums appear (reference Fig. (8)). Although these two minimums appear at this critical value, they do not become energetically favorable until a certain threshold value, r_T , is reached and thus the system will remain in the Sm-A phase. At the threshold value, the free energy of these two minimums drops lower than the free energy of the minimum at $c = 0$, and it now becomes energetically favorable for the system to be in the Sm-C phase. The minimum at $c = 0$ does not disappear until $r < 0$, which leads to some interesting behavior.

For $0 < r < r_c$, it is possible for the system to be in either the Sm-A or the Sm-C phase. Although the Sm-C minimums have a larger free energy when $r > r_T$, a small perturbation to the system could give the system enough energy to move over the “hump” and into a tilted state from the non-tilted state at $c = 0$. This would put the system in a Sm-C phase before reaching the actual threshold value. Similarly, as r is dialed

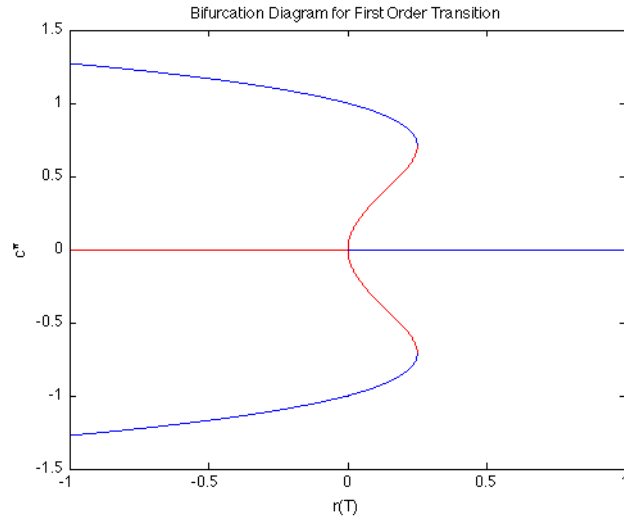


Figure 10: The fixed points plotted as a function of r for the first order phase transition. For simplicity, $u = -1$ and $v = 1$. The blue lines correspond to stable fixed points and the red corresponds to unstable fixed points. The value of r where a subcritical pitchfork bifurcation occurs is directly related to the transition temperature, T_c , of the liquid crystal.

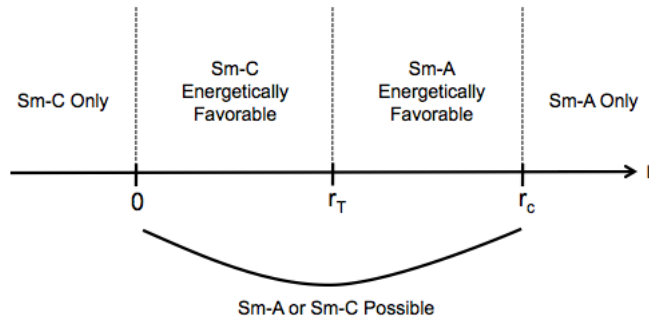


Figure 11: A one dimensional phase diagram for the first order transition showing the behavior of the system as r changes.

below r_T , unless the system experiences the same type of perturbation it may not have enough energy to go over the “hump” and into the lower energy tilted phase. This would mean the system would remain in the Sm-A phase even below the threshold value. To get a better visual idea of these “humps”, reference back to the free energy diagrams for different values of r in Fig. (8). The ability of the system to “jump” from one energy state to another at different temperature values (different values of r) is known as hysteresis. An important analogy to this behavior is the process of supercooling. The temperature of water can be lowered beyond the freezing point, yet still remain in

a liquid state. Like the liquid crystal, it must be given an extra "boost" of energy in order to jump into the lower energy solid state from the liquid state. However, if the temperature is lowered very slowly, and there is no presence of any sort of energetic perturbations, the liquid will remain past the freezing point. This is similar to the liquid crystal remaining in the Sm-A phase all the way down to $r = 0$.

Throughout the previous section, we have seen that smectic liquid crystals will undergo a phase transition from an average tilt of zero, to a nonzero tilt throughout. This happens by lowering the temperature of the system to some value of T_c . In a continuous phase transition, we see a supercritical pitchfork bifurcation at this critical point. The tilt of the molecules gradually increases as we lower temperature past this point. In a first order transition, we see the potential for hysteresis and a spontaneous jump in the tilting of the molecules near T_c , as is characteristic of a subcritical pitchfork bifurcation. In the next section, we will see how the application of an electric field can induce similar tilting behaviors in a liquid crystal cell while temperature is held constant. We will do this in a more quantitative way, whereas this section was meant to introduce the basic mathematical behavior of these phase transitions.

3 The Bulk Electroclinic Effect

Certain types of liquid crystals are chiral and contain a permanent dipole moment within their molecular structure. This characteristic results in ferroelectricity, which is a property of materials that allows an electric polarization to be induced by an external electric field. Due to these properties of the liquid crystal molecules we study, it is possible to induce the Sm-A* to Sm-C* (where * denotes the chirality) transition by applying an external electric field to a liquid crystal cell while maintaining a constant temperature above the critical temperature T_c . This is illustrated in Fig. (12).

When liquid crystal molecules are inserted between two electrodes, they form layers. In the absence of an applied electric field, the molecules will be in the Sm-A phase and no tilting will be present. As seen in Fig. (13), it is possible to apply an electric field to the right or the left. If we rotate the cell 90 degrees, we see that applying a field into or out of the page results in a tilt to the right or left respectively, a process called electro-optical switching. In this scenario, the bulk of the cell is now in an induced Sm-C phase and the average molecular tilt is no longer zero. The basic analysis of section 2 contained simple values for most of the parameters in order to simply illustrate the behavior of the system. From this section forward the behavior will be qualitatively similar, however we will use common experimental values for the parameters in order to compare our theoretical results to experimental results. In addition, plots will be made in terms of θ rather than c by the simple substitution of $\theta = \arcsin(c)$.

Due to the presence of the applied external electric field, it is necessary to introduce a new term to our original Landau Free Energy equation given in equation (1). This

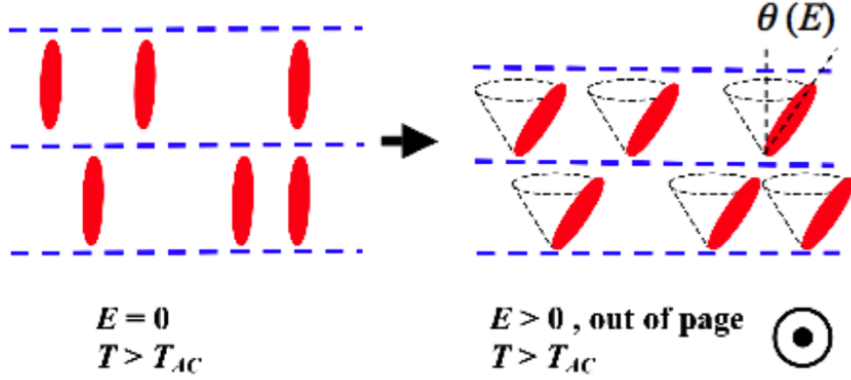


Figure 12: A Sm-A to Sm-C transition can be induced by applying an external electric field to a liquid crystal cell due to the ferroelectric properties of the chiral materials. This transition can occur while maintaining a constant temperature above T_c .

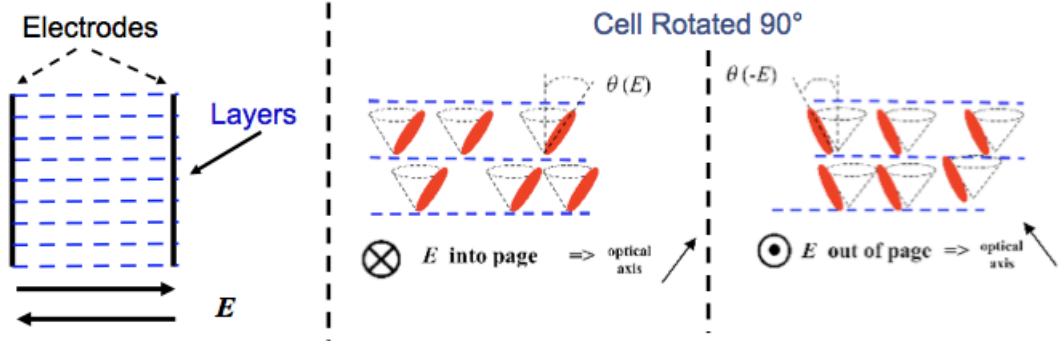


Figure 13: By applying an electric field into a cell from the left or right, it is possible to induce a tilting in the bulk of the liquid crystal molecules thus transitioning from a Sm-A to a Sm-C phase. Depending on which way the field is applied, the molecules will tilt in different directions, which is known as electro-optical switching.

equation now becomes:

$$F = \int \delta x \delta y \delta z \left[\frac{1}{2} A \tau(T) c^2 + \frac{1}{4} u c^4 + \frac{1}{6} v c^6 - D \chi E c \right] = V f(c), \quad (3)$$

where $D\chi$ is the coupling strength between the electric field E and the tilting of the molecules, given by the order parameter c , as before. The free energy density is now given by:

$$f(c) = \frac{1}{2} A \tau(T) c^2 + \frac{1}{4} u c^4 + \frac{1}{6} v c^6 - D \chi E c. \quad (4)$$

We can now minimize equation (4) with respect to c to determine the preferred tilt of the system for different values of E . Upon minimization, we obtain:

$$E = \frac{1}{D\chi}(A\tau(T)c + uc^3 + vc^5). \quad (5)$$

3.1 Continuous BECE

Equation 5 allows us to graph θ_B vs. E for multiple values of $u > 0$ at a value of $\tau = 0.1$ or 1% above the transition temperature. This can be seen in Fig. (14). As stated above, a system with a u value larger than zero will display a continuous Sm-A* to Sm-C*, therefore as we increase or decrease the value of external field E , there will only be one value of preferred tilt within the system. It has been established that many continuous Sm-A* to Sm-C* transitions occur at or near a tricritical point. In this scenario, the tricritical point occurs at $u = 0$, where the transition changes from continuous to first order. Therefore, u is a measure of how far the system is from this tricritical point. Thus, as u is decreased towards zero we see an increase in the susceptibility of the system and the electric field E has a greater effect on the tilt of the system.

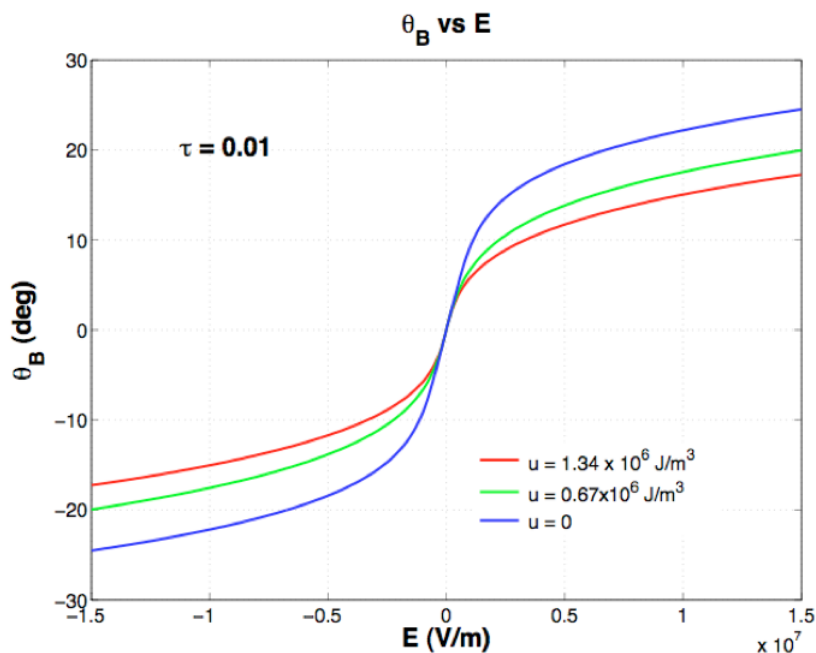


Figure 14: θ_B vs. E curves at a reduced temperature $\tau = 0.1$ for different values of u . The susceptibility of the system increases as we approach tricriticality at $u = 0$.

3.2 First Order BECE

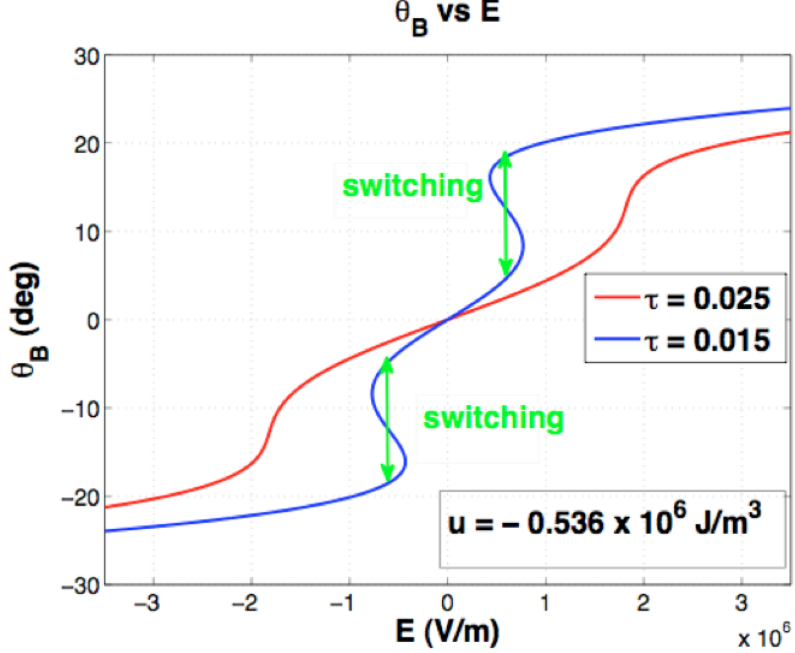


Figure 15: θ_B vs. E curves for different values of reduced temperature τ at a value of $u = -0.536 \times 10^6 \text{ J/ (m}^3 \text{ rad}^2)$. For large τ the curve is single valued, but for $\tau_{1st} < \tau < \tau_{CB}$ the curve is multivalued, thus the system will jump between high and low tilts.

The first order Sm-A* to Sm-C* transition is much more complicated to analyze. The θ_B vs. E curves for different values of $\tau > \tau_{1st}$ and a u value of $-0.536 \times 10^6 \text{ J/ (m}^3 \text{ rad}^2)$ are shown in Fig. (15). We ensure $\tau > \tau_{1st}$ so that the system is in the Sm-A* phase before the application of an external field. For sufficiently large values of $\tau > \tau_{CB}$, the curve is still single valued. The Sm-C* to Sm-C* transition will occur continuously. At values of $\tau_{1st} < \tau < \tau_{CB}$ the situation is more complicated. In this situation, the curve becomes multivalued. This means that at certain values of electric field, there are two possible values of tilt, a low tilt c_{BL} and a high tilt c_{BH} . As the electric field is ramped up from zero, the system will initially be in the low tilt state. Once a threshold value of electric field E_T is reached, the system will jump to the higher tilt state which is now more energetically favorable.

It is possible to find the temperature dependence of $E_T(\tau)$ by recognizing that the bulk tilt will jump from c_{BL} to c_{BH} (or vice versa) when the condition $f(c_{BL}) = f(c_{BH})$ is satisfied, where $f(c_B)$ is given by equation (4). This allows for the construction of a phase diagram in $E - \tau$ space which can be seen in Fig. (16). The solid middle line corresponds to a line of Sm-C* - Sm-C* transitions from low to high tilt for each value

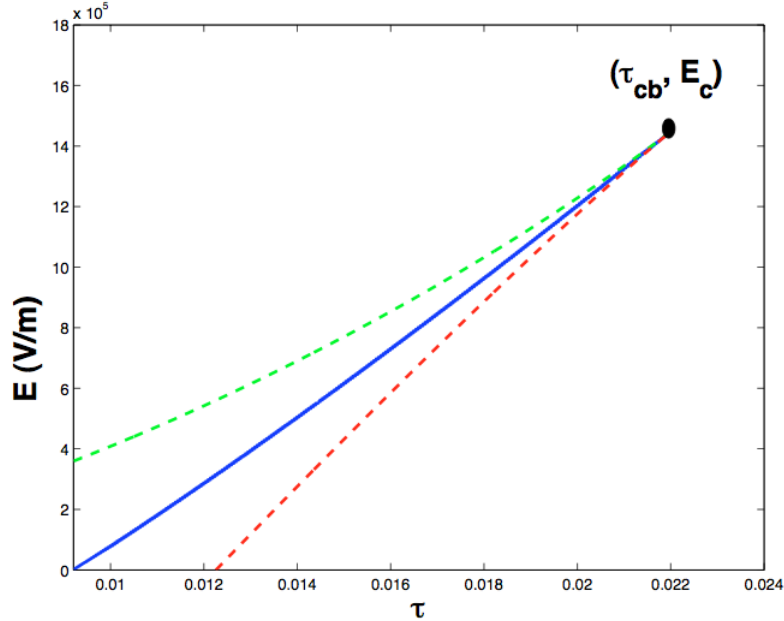


Figure 16: A phase diagram in $E - \tau$ space for the bulk tilt of a system displaying a first order transition. The solid blue line $E_T(\tau)$ corresponds to a line of Sm-C* to Sm-C* transitions from lower tilt to higher tilt. The upper and lower dashed lines represent the metastability boundaries, E_U and E_L respectively. Between these lines the bulk tilt is multivalued and may display hysteresis.

of τ . $E_T(\tau)$ spans from τ_{1st} to τ_{CB} , which is the width of the multivalued region. The upper and lower dotted lines correspond to the upper and lower electric field values (E_U and E_L respectively) for which the multivalued region begins and terminates at each value of τ . Within this multivalued region, both high tilt and low tilt states are possible. Above the $E_T(\tau)$ line, the high tilt state is energetically favorable while below $E_T(\tau)$ the low tilt state is energetically favorable. It isn't until E_U or E_L , however, that the system will actually be forced to move in to the high/ low tilt state respectively. In the absence of small energy fluctuations, the system will display a hysteresis loop equal to the width of the multivalued region.

4 The Surface Electroclinic Effect

When a liquid crystal is in contact with a surface, the interaction creates a localized effective field which causes behavior similar to the BECE at the surface. This phenomenon is called the surface electroclinic effect (SECE). The surface electroclinic effect is present whenever a liquid crystal is in contact with a surface regardless of whether or not an

external electric field is applied. This is due to the coupling of the dipole moments of the molecules to the treatment of the surface. The SECE by itself creates a localized tilting of the molecules at the surface, which relaxes back to align along the layer normal in the bulk. A schematic of this can be seen in Fig. (17). The direction of the tilting at the surface, c_S , is given by the director \hat{n} . This direction is chosen by rubbing the glass plates with a material that creates grooves and is called the "rubbing direction" \hat{R} . At the surface, \hat{n} and \hat{R} are parallel but become disaligned in the bulk.

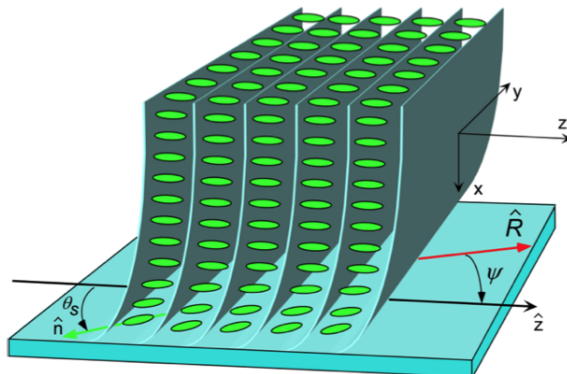


Figure 17: When a liquid crystal is in contact with a surface, a coupling occurs between the surface and the dipole moments of the molecules, which induces a non-zero tilt c_S at the surface. This occurs in the absence of an applied electric field and the molecules will relax back to align along the layer normal in the bulk.

Since the molecules are tilted at the surface and relax back as we move into the bulk of the cell, we must add an extra position-dependent term into our free energy density as well as the effective surface field term to our total free energy. In the absence of an applied electric field, the free energy of our system now becomes:

$$\frac{F}{A_{\perp}} = \int \partial x \left[\frac{1}{2} A \tau(T) c^2 + \frac{1}{4} u c^4 + \frac{1}{6} v c^6 + \frac{1}{2} K \left(\frac{dc}{dx} \right)^2 \right] - V_s e c(x=0), \quad (6)$$

where we take $V_s e$ to be w , the effective surface field which is proportional to a surface voltage (V_s) and the enantiomeric excess of the system (e). K is the twist elastic constant and A_{\perp} is the surface area of the glass plate of the cell and is used to simplify the integrals. Since the tilt of the system is now dependent on x , we must minimize equation (4) in order to find the tilt profile $c(x)$.

4.1 The Euler - Lagrange Equation

The Euler-Lagrange equation is a very important aspect of the calculus of variations and we will use it here in order to find the tilt profile of our system. This will allow us to extract important information about the behavior of the surface electroclinic effect. The integral in equation (4) is of the form:

$$\frac{F}{A_{\perp}} = \int_{x=0}^{x=\infty} f(x, c(x), c'(x)) dx - wc(x=0), \quad (7)$$

and satisfies the conditions $c(x=0) = c_S$ and $c(x=\infty) = c_B$, the tilt at the surface and in the bulk respectively. In the case of only the surface electroclinic effect, the molecules relax back to align along the layer normal as we extend into the bulk, which means $c_B = 0$. We keep c_B throughout the following analysis, however, so that the same analysis can be applied to a more complicated situation later on. For an integral of this form, the Euler - Lagrange equation is as follows:

$$\frac{\partial f}{\partial c} = \frac{d}{dx} \left[\frac{\partial f}{\partial c'} \right], \quad (8)$$

where

$$f = \frac{1}{2}A\tau(T)c^2 + \frac{1}{4}uc^4 + \frac{1}{6}vc^6 + \frac{1}{2}K \left(\frac{dc}{dx} \right)^2. \quad (9)$$

Since f has no explicit dependence on x , we are able to use the Beltrami identity, which is associated with the Euler- Lagrange equation. The Beltrami identity is:

$$f - \left(\frac{dc}{dx} \right) \left(\frac{\partial f}{\partial c'} \right) = H \quad (10)$$

where H is just a constant. By applying this formula to equation (9) we obtain:

$$f_u(c) - \frac{1}{2}K \left(\frac{dc}{dx} \right)^2 = H \quad (11)$$

where $f_u(c)$ or “f uniform” is the free energy density when the tilt is uniform given in equation (2). We can now use the fact that in the bulk of the cell, $\frac{dc}{dx} = 0$ and $f_u(c) = f_u(c_B)$ to rewrite equation (11) as:

$$f_u(c) - \frac{1}{2}K \left(\frac{dc}{dx} \right)^2 = f_u(c_B). \quad (12)$$

By solving for $\frac{dc}{dx}$, taking the negative root (since tilt decreases into bulk), and solving the separable differential equation, we obtain:

$$x = \int_{c(x)}^{c_S} \frac{dc}{\sqrt{\frac{2}{K} [f_u(c) - f_u(c_B)]}}. \quad (13)$$

This would allow us to obtain the tilt profile $c(x)$, however we first need to know the preferred tilting at the surface, c_S . In order to find the c_S that minimizes the equation, we must go back and apply the Euler Lagrange equation to equation (4). If we then do a change of variables and minimize, we obtain the useful expression:

$$f_u(c_S) = f_u(c_B) + \frac{w^2}{2K}. \quad (14)$$

4.2 θ_S vs. w

In the absence of an applied electric field, $f_u(c_B) = 0$ and equation (14) becomes significantly more simple. This expression now allows us to obtain plots for the w dependence of θ_S . For the continuous case, as seen in Fig. (18), we have plotted θ_S vs. w for three different values of u at one percent above the transition temperature. As was the case with the bulk tilt, we can see that the surface tilt increases continuously with w and is more susceptible the closer we are to the tricritical point at $u = 0$. For the first order case, as seen in Fig. (19), we have plotted θ_S vs. w for three different values of τ and used $u = -0.536 \times 10^6 \text{ J/ (m}^3 \text{ rad}^2)$. For sufficiently large values of τ the curve remains single valued. When we start to decrease τ towards the transition temperature, we see that our curves become multivalued giving us the possibility of surface tilt jumping and hysteresis at a certain value of $w = w_T$.

As with the BECE, it is possible to obtain a state map in $w - \tau$ space that demonstrates the temperature dependence of w_T for a first order transition. This is done by comparing the free energies of the low and high tilt states and finding where they are equal. Although a similar process was used, the need to integrate the spatially dependent free energy of the SECE makes this state map a little more difficult to obtain. It can be seen in Fig. (20). While the solid line represents $w_T(\tau)$, the dashed lines correspond to the upper and lower metastability limits w_U and w_L . Between these boundaries, the surface tilt is multivalued and may display hysteresis. w can be varied by changing the enantiomeric excess of the system, however varying the enantiomeric excess also impacts the transition temperature. This complication is discussed in further detail in our publication [2]. In this paper, varying w is understood to correspond to varying V_s via the treatment of the surface rather than the enantiomeric excess.

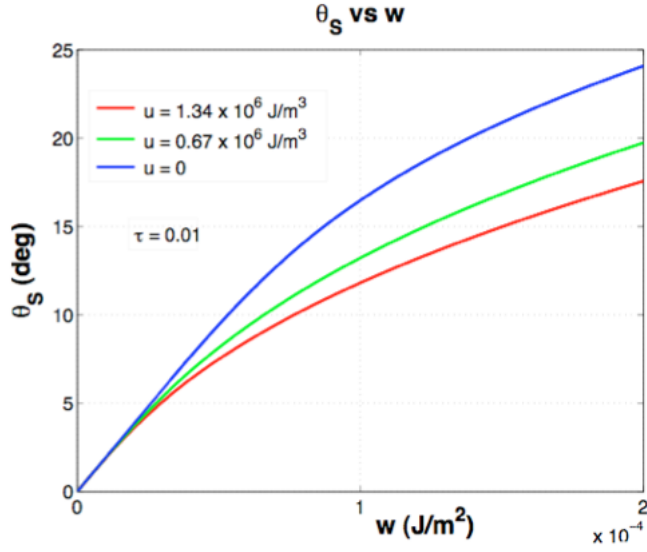


Figure 18: θ_S vs. w curves at a reduced temperature $\tau = 0.1$ for different values of u . The susceptibility of the system increases as we approach tricriticality at $u = 0$.

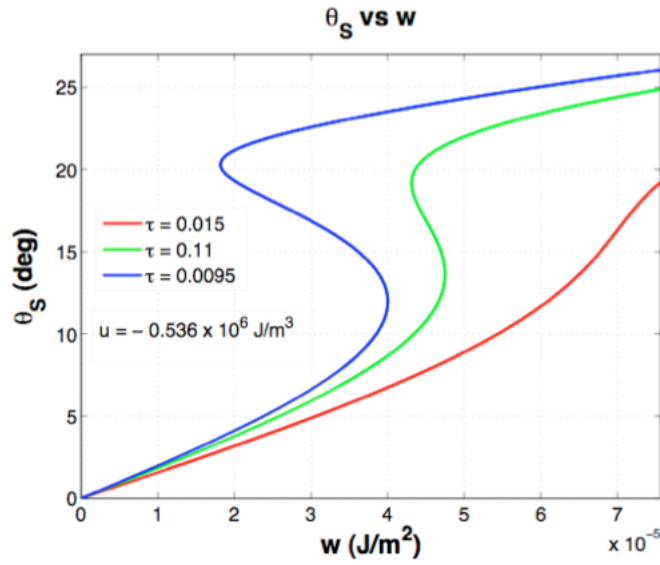


Figure 19: θ_S vs. w curves for different values of reduced temperature τ at a value of $u = -0.536 \times 10^6 \text{ J}/(\text{m}^3 \text{ rad}^2)$. For large τ the curve is single valued, but for $\tau_{1st} < \tau < \tau_{cs}$ the curve is multivalued, thus the system will jump between high and low tilts.

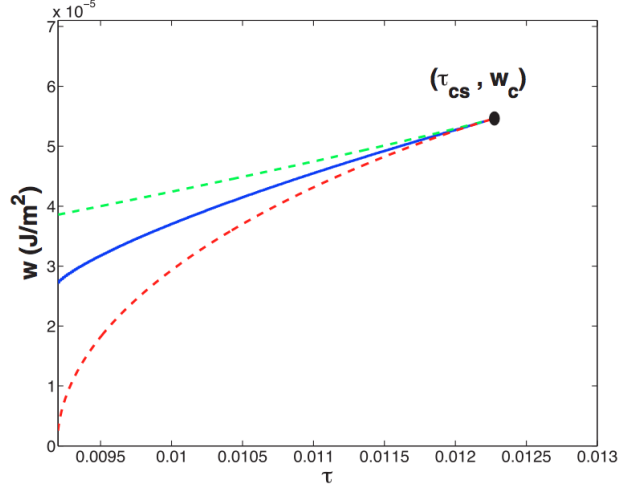


Figure 20: A phase diagram in $w - \tau$ space for the surface tilt of a system displaying a first order transition. The solid blue line $w_T(\tau)$ corresponds to a line of Sm-C* to Sm-C* transitions from lower tilt to higher tilt. The upper and lower dashed lines represent the metastability boundaries, w_U and w_L respectively. Between these lines the bulk tilt is multivalued and may display hysteresis.

5 Field Control of the SECE

After studying both the BECE and the SECE independently, we wanted to theoretically investigate whether or not we can control the surface tilt by applying an external electric field. An experimental group at the University of Colorado found that it is possible to vary the amount of surface tilt by applying an electric field opposite the surface field w as the smectic layers are forming [3]. Here we present the theory.

In order to model both the surface and bulk electroclinic effects together, we must now introduce the electric field term from equation (3) into equation (4). This gives us our total Landau free energy:

$$\frac{F}{A_{\perp}} = \int \partial x \left[\frac{1}{2} A \tau(T) c^2 + \frac{1}{4} u c^4 + \frac{1}{6} v c^6 - D \chi E c + \frac{1}{2} K \left(\frac{dc}{dx} \right)^2 \right] \quad (15)$$

$$- V_s e c(x=0),$$

The analysis of the previous section still holds, however $f_u(c)$ is now given by equation (4), since $E \neq 0$ and we can no longer ignore the electric field term. We must now use equation (14) in its entirety since c_B is no longer zero.

5.1 Continuous Transition

In order to find the electric field dependence of the surface tilt, extensive numerical computation was done. We fixed the effective surface field at a negative value of w for experimental comparison. For a large array of possible bulk tilt values, we obtained the corresponding electric field values (E) and bulk free energy densities (equation (4)). Choosing $c_S > c_B$, we looped through an array of possible c_S values in order to find the one which satisfies equation (14). Through this process we were able to obtain an array of surface tilts and their corresponding electric field value, plotted in figure (21).

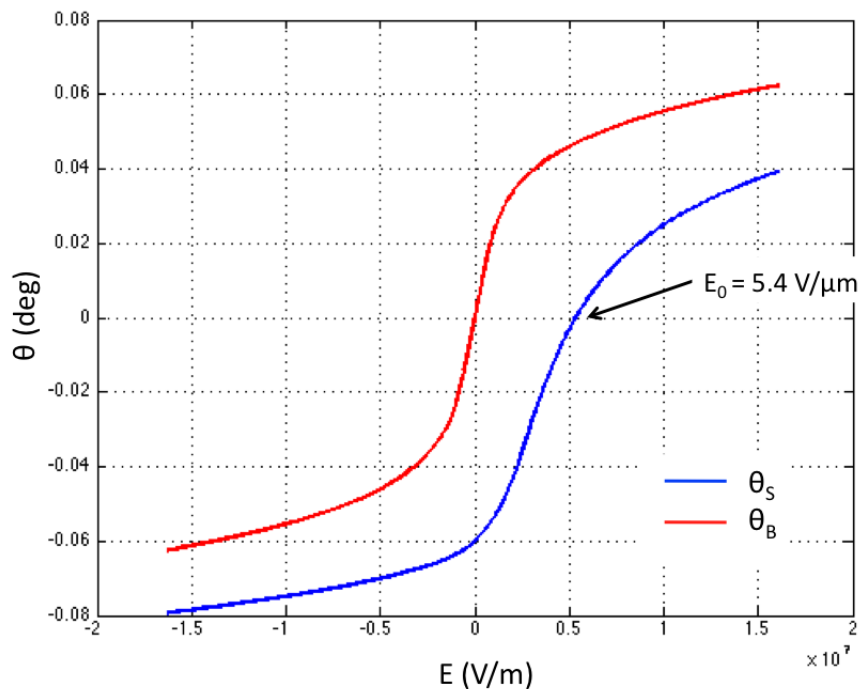


Figure 21: θ_S vs. E for a continuous transition with $w < 0$. Both θ_S and θ_B increase continuously with the application of an external electric field. The value of electric field that eliminates the surface tilt completely was found to be $\approx 5.4 \times 10^6$ V/m.

As seen from Fig. (21), both the bulk and surface tilts increase and decrease continuously with electric field variations. Since $w < 0$, the surface tilt is negative for $E = 0$. At a value $E_0 \approx 5.4 \times 10^6$ V/m. the surface tilt has been completely eliminated.

5.2 First Order Transition

We were also able to obtain θ_S vs. E for a first order transition using a similar numerical method. As with the bulk tilt, the surface tilt also has the potential to jump and display

hysteresis for certain values of electric field. The results are plotted in Fig. (22) for three different values of τ . As seen from Fig. (16) and (20), $\tau_{cs} < \tau_{cb}$ which means that the surface tilt will become discontinuous at a lower temperature than the bulk tilt. In Fig. (22a), $\tau > \tau_{cb}$ and both $\theta_S(E)$ and $\theta_B(E)$ are continuous. In Fig. (22b), $\tau_{cs} < \tau < \tau_{cb}$. Here we see that the bulk tilt has become discontinuous and the surface tilt remains continuous, however there is a kink in $\theta_S(E)$ where the bulk tilt jumps. When dealing with this situation numerically, it is important to ensure that the lowest energy θ_B value is used to determine θ_S . In Fig. (22c), $\tau < \tau_{cs}$ and we see that both $\theta_S(E)$ and $\theta_B(E)$ are discontinuous. We must be careful to use the lowest energy θ_B in this situation as well.

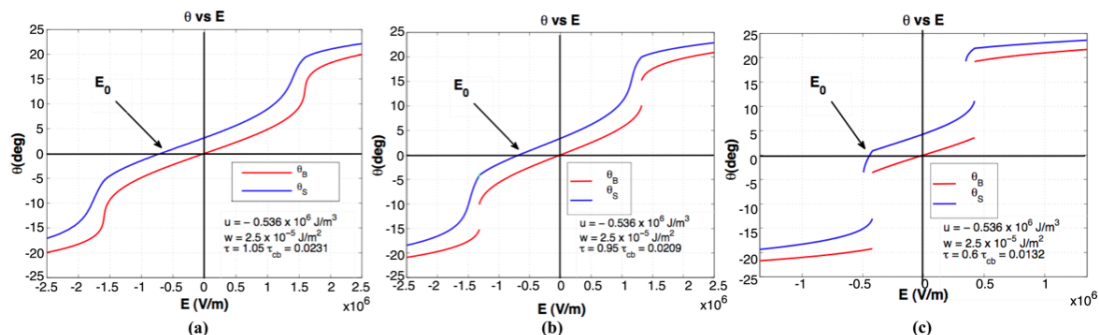


Figure 22: θ_S vs. E for a first order transition and $w > 0$.

6 Layering Effects

6.1 A Qualitative Analysis of the Continuous Transition

A significant consequence of being able to control the surface tilt with an applied electric field is that the tilt of the molecules at any given value of E will differ between the surface and the bulk. This can be seen above in Fig. (21) where we plot θ_S and θ_B vs. E for a continuous transition. Similar to the concept first introduced in section 2, the tilting of the molecules in the bulk or at the surface will result in a different preferred layer spacing in the bulk or at the surface. This preferred layer spacing is given by $d = d_0 \cos(\theta)$ where d_0 is the layer spacing at zero tilt. For $w < 0$, it is useful to investigate different regions based upon the value of applied electric field in order to further understand what is going on in terms of the layers. It is also important to note that the following analysis will consider the effect of the tilting on the layer spacing and not the effect of the layer spacing on the molecules. A full analysis would consider both of these effects equally, however that is beyond the scope of this paper.

6.1.1 $E \leq 0$

When $E \leq 0$, the magnitude of the tilt at the surface is greater than the magnitude of tilt in the bulk. This can be seen both two-dimensionally and three-dimensionally in Fig. (23). In this scenario, the preferred layer spacing at the surface is smaller than the preferred layer spacing in the bulk. Since the layers first form at the surface, this difference in spacing creates a region of compressive strain with the liquid crystal cell. In order to relieve this compressive strain, the cell will remove layers in the bulk via edge dislocations and thus a larger average spacing will be present in the bulk of the cell. A schematic of this situation can be seen in Fig. (24). Edge dislocations occur close to the surface and thus result in a relatively well-aligned bulk within the cell.

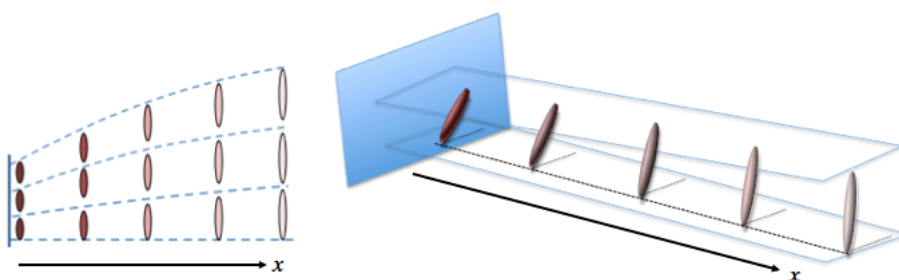


Figure 23: When $E \leq 0$, the magnitude of θ_S is greater than the magnitude of θ_B . This means that the preferred layer spacing is smaller at the surface and creates a region of compressive strain.

6.1.2 $E \geq E_0$

As stated above, E_0 is the value of electric field for which the surface tilt has been completely eliminated. For field values larger than this special value, the magnitude of the surface tilt θ_S is smaller than the magnitude of the bulk tilt θ_B . This means that the preferred layer spacing at the surface is now larger than the preferred layer spacing in the bulk, which results in a region of dilative strain. A schematic can be seen in Fig. (25). Dilative strain can also be relieved by the formation of edge dislocations, however now the edge dislocations are present to form new layers within the bulk. This results in a smaller average layer spacing in the bulk, where the molecules experience a higher amount of tilting. In addition to edge dislocations, however, dilative strain can also be relieved by a buckling of the layers. This undulation of the layers results in a larger average layer spacing and is thus able to relieve the strain. Both of these possibilities are illustrated in Fig. (26), however layer buckling tends to be more energetically favorable in this scenario [4].

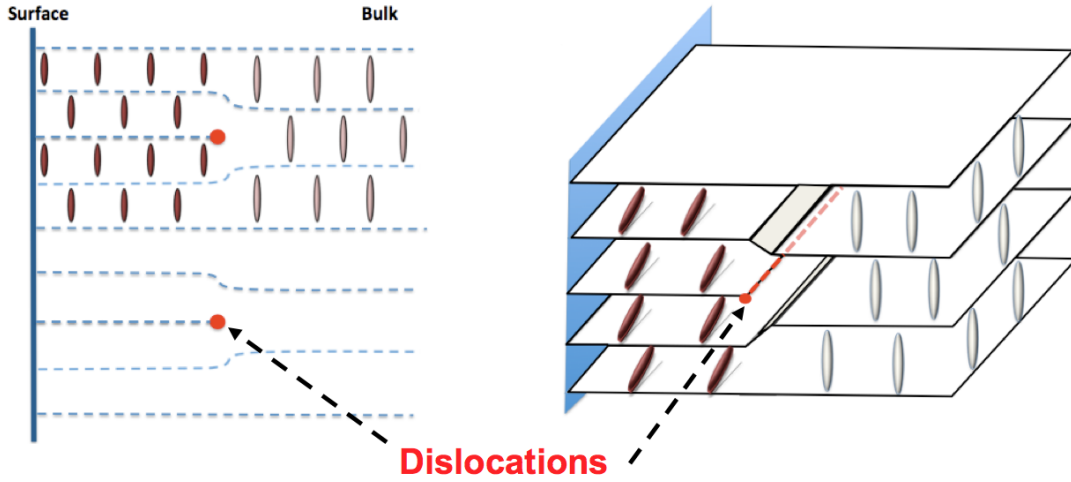


Figure 24: Compressive strain can be relieved via edge dislocations, which remove layers as we extend into the bulk, allowing for a larger average layer spacing to account for the less tilted bulk molecules.

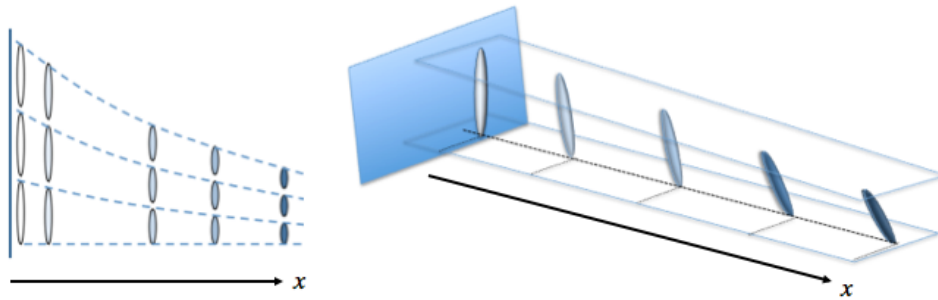


Figure 25: When $E \geq E_0$, the magnitude of θ_S is smaller than the magnitude of θ_B . This means that the preferred layer spacing is larger at the surface and creates a region of dilative strain.

6.1.3 $0 < E < E_0$

When the applied electric field falls within this region, the situation gets a little more complicated. The molecules at the surface and in the bulk now tilt in opposite directions since a slightly positive field will make the surface tilt less negative and the bulk tilt positive. This means that the system will have a region of compressive strain at smaller x and a region of dilative strain at larger x . This is shown schematically in Fig. (27). Since compressive strain can only be relieved by dislocations, we expect these to occur in the region of smaller x while in the dilative region we could potentially have dislocations or

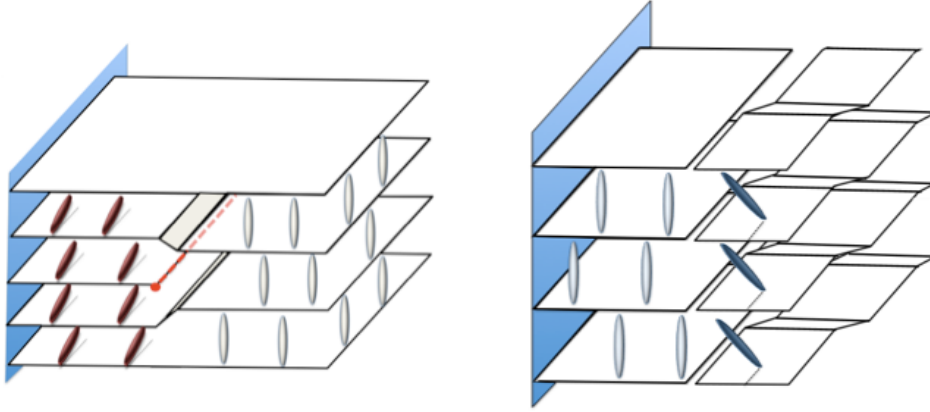


Figure 26: Dilative strain can be relieved by adding layers via edge dislocations as we extend into the bulk or by the buckling of the layers in the bulk, which creates a larger average layer spacing in the bulk.

buckling. Both of these scenarios are shown in Fig. (28). Determining which of these is energetically favorable is beyond the scope of this paper, however based on experimental results, we suspect that it will be dislocations only. We call this the intermediate region and will make a few more comments on its significance in the following section.

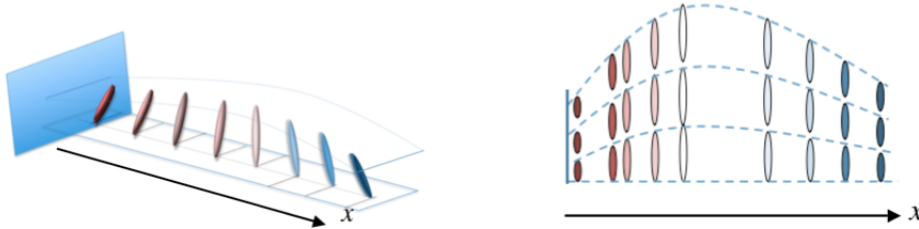


Figure 27: When $0 < E < E_0$, θ_S and θ_B have opposite signs, thus causing a region of compressive strain at smaller x and a region of dilative strain at larger x .

7 Strain: Quantifying Layer Effects

The previous section investigates the qualitative effects of differences in surface and bulk tilting. This section will introduce a quantitative analysis by defining and looking at the strain in cells that display this behavior. In doing this we hope to explain the significant drop offs in alignment quality seen experimentally in regions of dilative strain [3]. This experimental drop off appears to occur right around the value of applied electric

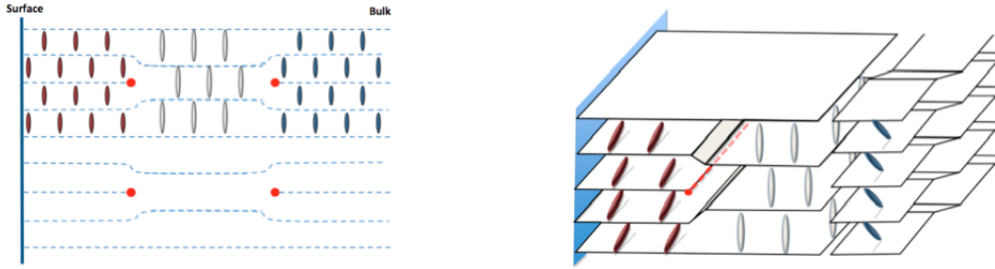


Figure 28: Since compressive strain can only be relieved via dislocations and dilative strain can be relieved with dislocations or layer buckling, we propose two potential schematics for strain relief in the intermediate region.

field which totally eliminates the surface tilt, which we have found theoretically to be $\approx 5.4 \times 10^6$ V/m.

In their 1973 paper [4], Noel Clark and Bob Meyer found that pulling apart the top and bottom plates of a simple non-chiral Sm-A liquid crystal cell caused a dilation of the layers from their preferred spacing. In this situation, the layers are forced to have a spacing larger than their preferred spacing. In regions of dilative strain, dislocations or buckling may occur. The displacement of the layers is given by:

$$u(x, z) = \alpha z + u_0 \cos(q_1 x) \cos(q_3 z), \quad (16)$$

where q_1 is the buckling wave vector and is equal to $2\pi/\lambda$. The $\cos(q_3 z)$ term ($q_3 = \pi/d$) is required to satisfy boundary conditions at the top ($z = d/2$) and bottom ($z = -d/2$) plates, and α is the dilative strain. The magnitude of the strain due to an imposed layer spacing d is

$$\alpha = 1 - \frac{d_p}{d} \quad (17)$$

where d_p is the preferred spacing of the system. In regions of compressive strain, $\alpha < 0$ and in regions of dilative strain, $\alpha > 0$. In regions of dilative strain it can be shown that the threshold strain for the onset of buckling is given by

$$\alpha_T = \frac{2\pi}{L_z} \left(\frac{K_1}{B} \right)^{\frac{1}{2}} \quad (18)$$

where L_z is the height of the cell, B is the smectic bulk modulus and K_1 is the smectic bend modulus. If we plug in typical experimental values for these parameters [4] we find that $\alpha_T \approx 10^{-4}$.

In the Clark-Meyer analysis, they were able to induce a non-zero strain in the cell by moving the top and bottom plates, and thus changing d . In our analysis, we consider fixing the top and bottom plates (and thus d) and then changing d_p by having the molecules tilt through the bulk electroclinic effect. In both cases, the layer spacing d is larger than the preferred spacing d_p , and thus a similar analysis applies and we can use the same α_T . For the Sm-A* to Sm-C* transition, $d = d_S$ since upon cooling into the Sm-A* phase, the layers first nucleate at the surface and then extend into the bulk. The preferred spacing of the system is position dependent since the tilt varies as we go from the surface to the bulk. The preferred layer spacing of the system d_p , as seen schematically in Fig. (3), is given by

$$d_p(x) = d_A \cos(\theta_p(x)) \quad (19)$$

where d_A is the spacing in the Sm-A phase when no tilting is present (the maximum possible spacing). Using equations (17) and (19) we can obtain a position dependent strain

$$\alpha(x) = 1 - \frac{d_p(x)}{d_S} = 1 - \frac{\cos(\theta(x))}{\cos(\theta_S)} \quad (20)$$

where $\theta(x)$ can be found using equation (13). The max strain within the system at any given time can be found using

$$\alpha_{max}(E) = 1 - \frac{\cos(\theta_B)}{\cos(\theta_S)}. \quad (21)$$

Using equation (21), we can plot the maximum strain versus our electric field which can be seen in Fig. (29). From this figure, our theoretical value of $\alpha_T \approx 10^{-4}$ for the onset of buckling yields an electric field value of $E_T \approx 2.5 \times 10^6$ V/m. Experimentally, however, E_T was found to be $\approx 5.4 \times 10^6$ V/m and was approximately equal to the electric field value for which the surface tilt was completely eliminated, E_0 .

For a possible explanation of the discrepancy between these two values of E_T we turn to Fig. (30). In the previous section we introduced the possibility of three different regions based on the applied electric field. For $E < 0$, we are in a region of purely compressive strain and can only relieve this strain with dislocations. For $E > E_0$, we are in a region of purely dilative strain and can relieve this strain with either dislocations or buckling, however buckling is more energetically favorable. The intermediate region, for $0 < E < E_0$, contains both dilative and compressive strain. In this region, we proposed two different ideas for strain relief: a pair of dislocations and a dislocation-buckling scenario. Since dislocations occur relatively close to the surface, the bulk of the cell remains comparatively well aligned. Although it is theoretically possible to have

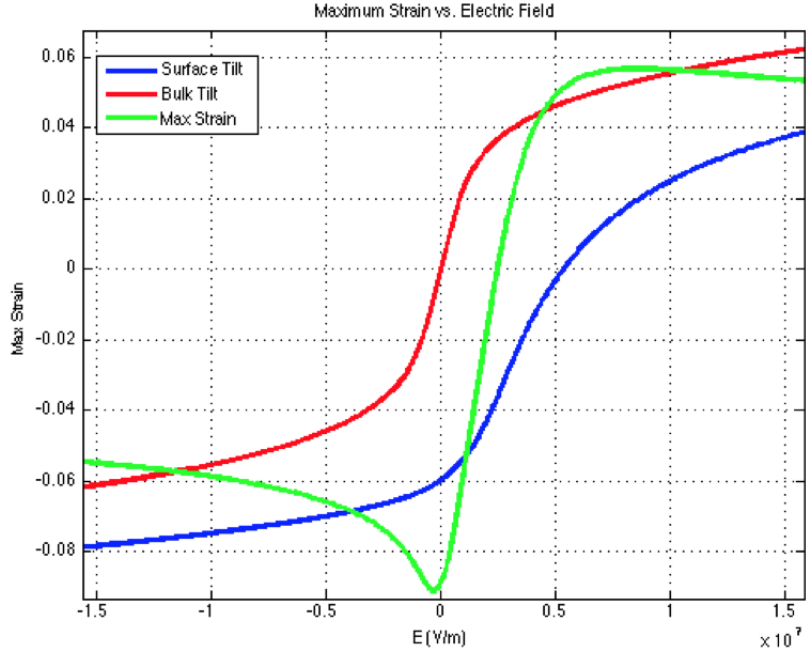


Figure 29: Max strain versus electric field for a continuous transition.

buckling around a value of $E_T \approx 2.5 \times 10^6$ V/m within this region, we do not see a drop off in alignment quality until a value of $E_0 \approx E_T \approx 5 \times 10^6$ V/m.

Although the energetics of dislocations vs. buckling in the intermediate region are beyond the scope of this project, we propose that the onset of buckling will not occur unless we are in a region of purely dilative strain, $E > E_0$.

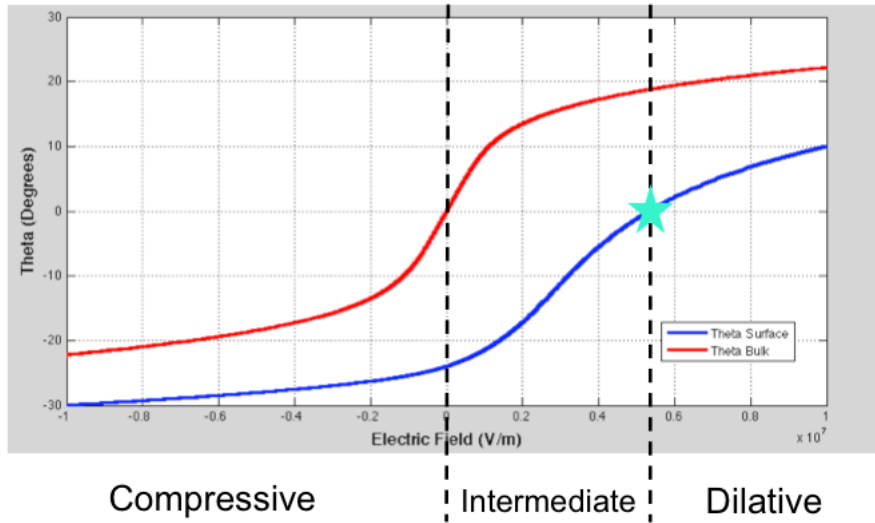


Figure 30: The different regions of strain within a LC cell based on differing surface and bulk tilts for a span of electric field values. For $E < 0$ strain is compressive, for $E > E_0$ strain is dilative, and for $0 < E < E_0$ we are in an intermediate region where both compressive and dilative strain are present.

References

- [1] Collings, P. J. (1990). *Liquid crystals: nature's delicate phase of matter* (1st ed.). Princeton, N.J.: Princeton University Press.
- [2] K. Zappitelli, D. Hipolite and K. Saunders, Phys. Rev. E. **89**, 022502 (2014).
- [3] J. E. Maclennan, D. Muller, R.-F. Shao, D. Coleman, D. J. Dyer, D. M. Walba and N. A. Clark, Phys. Rev. E. **69**, 061716 (2004)
- [4] N. A. Clark and R. B. Meyer, Appl. Phys. Lett. 22, 493 (1973).